ADVANCED FUNCTIONAL MATERIALS
www.afm-journal.de

Materials Views
www.MaterialsViews.com

An Individual Carbon Nanotube Transistor Tuned by High Pressure

By *Christophe Caillier, Anthony Ayari, Vincent Gouttenoire, Jean-Michel Benoit, Vincent Jourdain, Matthieu Picher, Matthieu Paillet, Sylvie Le Floch, Stephen T. Purcell, Jean-Louis Sauvajol,* and *Alfonso San Miguel**

A transistor based on an individual multiwalled carbon nanotube is studied under high-pressure up to 1 GPa. Dramatic effects are observed, such as the lowering of the Schottky barrier at the gold–nanotube contacts, the enhancement of the intertube conductance, including a discontinuity related to a structural transition, and the decrease of the gate hysteresis of the device.

1. Introduction

During the last decade, many efforts have been devoted to integrate carbon nanotubes (CNT) in nano-electronic applications. This means not just using nanotubes collectively in networks, mats or composite materials, but also using individual nanotubes as the central components in devices. Indeed, beyond their nanoscale size and their huge capacity to transport current,[1] the particularity of CNTs compared to other bulk material is that they can be seen as building blocks of more complex structures, each individual tube having a precise function in the system. For example, a metallic CNT can become a quantum wire,[2] while a semiconducting CNT can act as a field effect transistor if gated.[3,4] The gate can even be a metallic CNT.[5] This gives rise to many perspectives for nanotube-based logic circuits.[6,7]

Additionally, many interesting nanotube-based electromechanical devices stem from their outstanding mechanical properties[8–10] among which are high resilience, high Young's modulus and an ability to support strong bending. As well they can readily be used as resonators[11–13] and their electronic properties can be influenced appreciably by strain.[14,15] In carbon nanotube-based devices, a single nanotube can even have several functions at the same time; for example, a radio based on one single nanotube serving as antenna, tunable band-pass filter, amplifier and demodulator has been reported.[16]

All these nanotube properties, and thus the performances of their devices, can be modified by stress-induced strain. In this context, pressure is one of the most interesting parameters, since besides a linear change of the electronic bandgap at low pressure,[17,18] it also induces at least two different transitions involving the nanotube cross-section[19,20] that can affect the CNT electronic properties.[21–25] These pressure-induced modifications of the electronic properties have been partially observed by photoluminescence on individualized nanotubes[26] and by transport measurements on nanotube networks.[27] Though encouraging, these results do not reveal all the interesting physics of the problem because they do not take into account the final geometry of the device, where only one nanotube is lying in contact with metal contacts.

To overcome this issue, the ideal case is thus to study the pressure evolution of the electronic properties on one individual contacted nanotube, without any surfactant, in an inert pressure-transmitting medium. Here we describe a setup to achieve such an experiment and the obtained results on an ambipolar transistor made of one individual contacted nanotube.

2. Results and Discussion

A scheme of the experimental setup is shown in **Figure 1a**. The substrate for the nanotube-device fabrication was a p++ doped silicon wafer, with a thermally grown silicon oxide layer of 300 nm. Gold electrodes were deposited by photolithography. The gold patterns were 300 nm thick and contained eight electrodes of 3 μm width separated by 1 μm. Carbon nanotubes were then grown directly on this substrate by chemical vapour deposition (CVD), with nickel particles as catalysts. As confirmed by more in-depth studies, this growth method generally gives individual nanotubes with few walls.[28] Here we will present the results obtained on one particular individual nanotube, which we will show to be at least double walled. A scanning electron microscopy (SEM) image shows the typical result (Figure 1c). However, no SEM was done on the present sample to avoid contamination. Instead, the presence of the nanotube was checked with a probe station, and its individual character was confirmed by atomic force microscopy (AFM; Figure 1d). Once the presence of the contacted nanotube was confirmed by its transport properties, the chip was fixed to the sample holder of the pressure chamber. Electrical contacts were made by gold wires and conductive epoxy polymerized at 120 °C. The nanotube was contacted in a transistor geometry with two contacts on the source-drain electrodes (voltage V_{sd}), where the nanotube

[*] Dr. Ch. Caillier, Dr. A. Ayari, Dr. V. Gouttenoire, Dr. J.-M. Benoit, Dr. S. L. Floch, Dr. S. T. Purcell, Prof. A. San Miguel
Université de Lyon
Laboratoire PMCN
CNRS, UMR 5586, Université Lyon 1, Villeurbanne 69622 (France)
E-mail: alfonso.san.miguel@univ-lyon1.fr
Dr. V. Jourdain, Dr. M. Picher, Dr. M. Paillet, Dr. J.-L. Sauvajol
Université Montpellier 2, CNRS UMR 5587
Laboratoire des Colloides Verres & Nanomat
Montpellier 34095 (France)

DOI: 10.1002/adfm.201000398

© 2010 WILEY-VCH Verlag GmbH & Co. KGaA, Weinheim

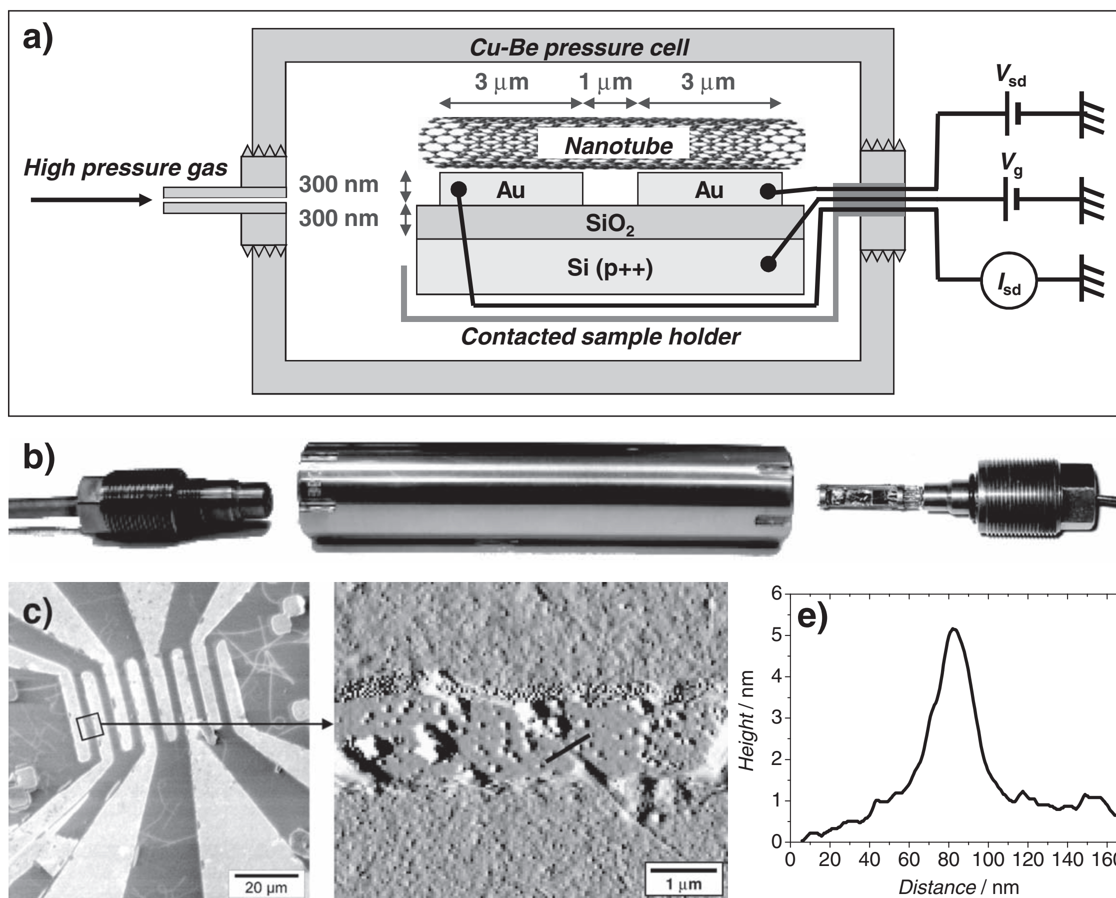

Figure 1. a) Scheme of the experimental setup to measure the transport properties of an individual carbon nanotube under high gas pressure (see text for details). b) Picture of the pressure cell featuring the body of the cell (center), the plug with the capillary tube (left) and the plug with the electrical feedthroughs and the contacted sample holder (right). c) Typical SEM image of the central part of a gold electrodes pattern with nanotubes grown on top. d) AFM image of the studied nanotube, crossing the inter-electrode gap (horizontal valley). No other nanotubes were observed crossing the gap elsewhere. Some particles, likely inactive catalysts, are visible inside the gap. e) Profile across the nanotube in the middle of the inter-electrode gap (black line in d). From this profile the diameter of the nanotube is estimated to about 4 nm.

was lying and one contact on the p++ doped silicon substrate for the gate voltage (V_g).

The pressure was applied by an automated three-stage gas compressor Unipress GCA-10, with argon as the pressure-transmitting medium. The sample holder was introduced inside a Cu–Be cylindrical pressure cell, connected to the gas compressor by a capillary tube at one of its extremities, and having electrical feedthroughs at the other extremity (Figure 1b). The pressure was measured from ambient pressure to 9.8 kbar by a manganin pressure gauge with a precision of about 50 bar. The experiment was carried out at ambient temperature.

The transport measurements were carried out using an automated computer program, with a National Instruments DAQmx 6211 to apply voltages with a precision of 0.5 mV and to measure the current (I_{sd}) flowing through the tube. The current was given by a transimpedance amplifier Keithley 427. For the present sample, the current I_{sd} was proportional to the source-drain voltage V_{sd} for all the gate voltages V_g. Therefore the interesting results were the I_{sd}–V_g characteristics for a given V_{sd}.

The principal experimental results are shown in **Figure 2**. At ambient pressure (Figure 2a), we observe an almost ambipolar transistor characteristic with a current that is non-zero in the middle of the gap. The pressure (P) dependence of the transport measurements are shown in Figure 2b, which shows a strong and monotonous dependence of the $I_{sd}(V_g)$ curve on P from 1 to 9.8 kbar. We observe a global increase of current and a symmetrization of the curves. It should be noted that this evolution is almost perfectly reversible, as later shown in Figure 2c and Figure 2d.

In order to quantify and understand this evolution, we must consider the nature of the tube that is measured. Using AFM (Figure 1d and 1.e), carried out after the pressure experiment, the nanotube diameter was estimated to approximately 4 nm. From this diameter, we conclude that the gap of the tube is either around 220 meV if it is a semiconductor (estimated from tight-binding calculations[29]), or less than 2.5 meV if it is metallic, because of curvature effects.[30] Since 2.5 meV is small compared to $kT = 25$ meV, the metallic hypothesis cannot explain the strong variation of current with V_g observed in Figure 2a. On the other hand, the curves are compatible with a gap of about 220 meV if we assume the presence of an inner metallic tube to account for the non zero current at $V_g = 1$ V. The nanotube is thus at least double walled, which in fact is the

© 2010 WILEY-VCH Verlag GmbH & Co. KGaA, Weinheim

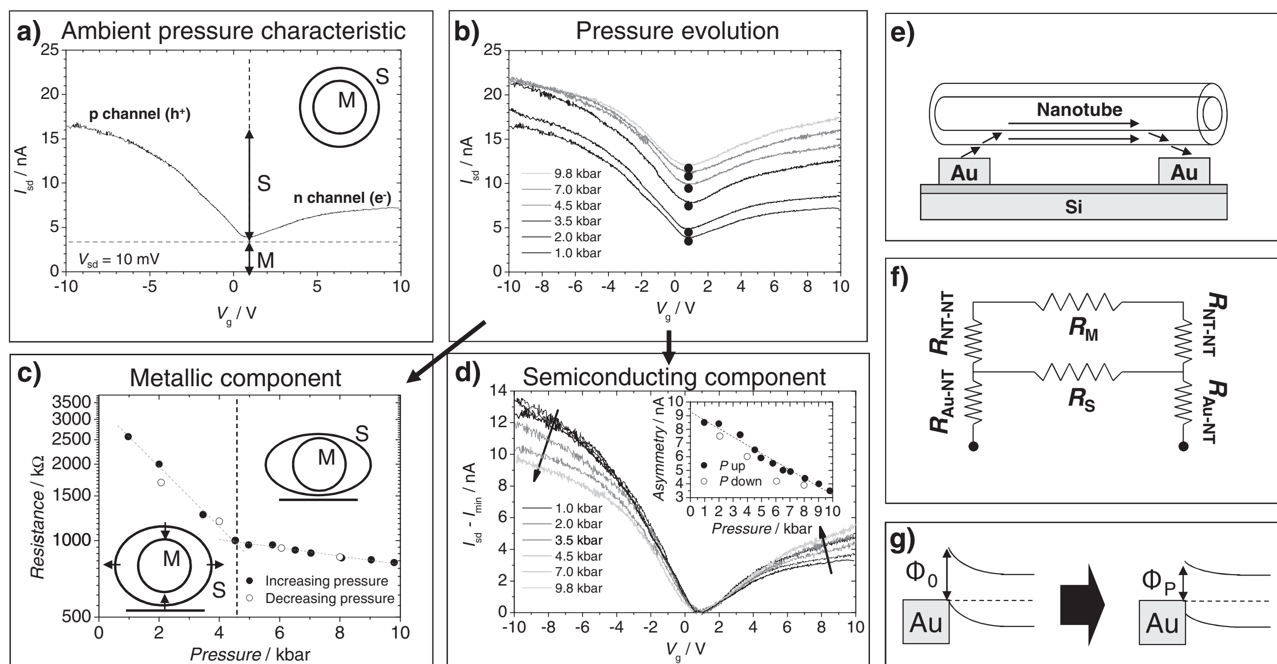

Figure 2. a) Current vs. gate voltage characteristics of the measured nanotube transistor at 1 kbar, with 10 mV as source-drain voltage. This curve is the average on V_g of the two hysteresis branches that are visible in Figure 3a. The transistor is ambipolar since both conduction with electron (positive gate voltage) and holes (negative gate voltage) are observed. This characteristic suggests that the CNT is a double wall nanotube (DWNT) in which the current is carried by two components: a metallic inner tube (M) and a semiconducting outer tube (S). This would be in agreement with the AFM measurements (Figure 1). See text for details. b) Pressure evolution of this characteristic from 1 kbar to 9.8 kbar. c) Pressure evolution of the resistance arising from the metallic component, i.e., resistance obtained by dividing the minimum current of (b) by the 10 mV source-drain voltage. A transition is observed at about 4.5 kbar. This transition is associated with a change of the nanotube cross-section evolution, as explained by the schemes and in the text. d) Pressure evolution of the semiconducting component, which is the curve of (b) minus its minimum. The transistor characteristic becomes more symmetric with pressure. This is confirmed by the decrease of the curve asymmetry (difference of current between $V_g = +10$ V and $V_g = -8$ V) plotted in inset. e) Simple scheme of the contacted nanotube indicating the path of electron flowing in the external semiconducting nanotube and in the internal metallic nanotube. f) Scheme of the equivalent circuit for the two nanotubes conducting in parallel. At the minimum of conduction (V_g close to 1 V), the resistance of the semiconducting nanotube (R_S) is supposed to become infinite compared to that of the metallic tube (R_M). g) Diagram of the electronic bands of the semiconducting nanotube near the gold contact. The energy difference between the conducting band of the nanotube and the Fermi level of the contact is the Schottky barrier height. The pressure causes this Schottky barrier height to decrease, resulting in the changes observed in (d).

most expected morphology for a 4 nm diameter nanotube.[31] Actually, in this side-contacted geometry, possible inner shells would not play a major role in the electronic transport because of the inter-shell resistance.[32] This also suggests that the metallic tube is inside the semiconductor, as it explains the low metallic contribution compared to the semiconducting one.

With this reasoning, we first studied the current flowing through the metallic nanotube at different pressures by following the minimum of the curves in Figure 2b. Figure 2c shows the resulting resistance R_{tot} vs. the applied pressure. Following the schema in Figure 2e and simple model in Figure 2f, and since the semiconducting tube is not conducting at the minimum, R_{tot} is the sum of R_{Au-NT} (gold–nanotube contact), R_{NT-NT} (inter-shell resistance), and R_M (the intrinsic resistance of the metallic tube). We observe a strong, nonlinear decrease of the resistance, which reaches a value more than three times smaller at 9.8 kbar than at 1 kbar. This resistance reduction is divided into two regimes separated by a clear break. From 1 to 4.5 kbar, the decrease is exponential, as shown by the straight line in the semi-log plot. From 4.5 to 10 kbar, the coefficient of the exponential decay is much lower. It can be approximated by a simple linear decrease of about – 3.1% $kbar^{-1}$, comparable to the resistivity decrease obtained along the graphite *c*-axis.[33]. The observed resistance decrease differs considerably from that of an individual metallic tube (unpublished data), which allows us to exclude the possibility that the system studied here corresponds to a small bundle. The observed behavior is fully reversible on pressure release, as seen in Figure 2c.

Let us here consider the pressure-induced mechanical transitions expected for CNTs of approximately 4 nm diameter that may be the cause of transition in the transport behavior. Calculations[19,34,35] and experiments[20,36] agree that the carbon nanotubes follow two consecutive transitions under hydrostatic compression. The first corresponds to a modification of the carbon nanotube cross-section from circular to oval (called "ovalization" in the following). The second corresponds to the deformation of the carbon walls into a peanut-like cross-section, where both sides of the tubes are attracted to each other, leading in particular to a strong hysteresis when the pressure is released. This second transition, usually called "collapse," implies a discontinuity in the flattening process. Both transitions are predicted to take place at pressures that scale as $1/d^3$, where d is the diameter of the tube, and they were actually observed in bundled nanotubes of 1.35 nm diameter at 23 kbar (2.3 GPa)

 © 2010 WILEY-VCH Verlag GmbH & Co. KGaA, Weinheim

and 140 kbar (14 GPa), respectively.[20] From these values and the $1/d^3$ law, we can predict ovalization and collapse transition pressures for the exterior 4 nm tube of around 0.8 and 5.4 kbar, respectively. In a DWNT these transitions should be pushed to higher pressures due to an additional mechanical support by the inner tube.[37–39] This supporting effect depends on the distance between the inner and outer tube. On the other hand, the interaction of a tube of 4 nm diameter with its substrate should lead to a reduction of the ovalization onset.[40] The absence of hysteresis during pressure release (see Figure 2c) allows us to exclude the collapse of the CNT as an explanation for the transition observed at 4.5 kbar. We can then reasonably consider two scenarios: i) ovalization takes place at 4.5 kbar, or, ii) the initial inter-tube distance at ambient conditions was larger than the graphitic one, so as to justify an ovalization of the outer tube at very low pressures (around 0.8 kbar). In such a case, the transition can be interpreted as the result of contact between the outer tube and the inner tube. Such a process is also known to explain the two-step pressure evolution of the G Raman band evolution for a double walled nanotube with a large inter-shell distance.[41,42] Moreover ovalization can explain the strong decrease of the resistance before 4.5 kbar through the rapid decrease of the intertube minimal distance.

From a practical point of view these results show that we can sensitively tune the current flowing in the inner tube by applying pressure. The high sensitivity of the effect,means that it is of interest for pressure sensing applications, though its calibration may require nanotubes of determined diameters.

Next, in order to study the -pressure evolution of the outer semiconducting shell alone, we can again plot the I_{sd}–V_g curves after subtraction of the metallic component. This is done in Figure 2d, where we clearly see that the effect of pressure is to reduce the p conduction channel and enhance the n channel. This effect is quantified in the inset of Figure 2d, where the difference between the p type current and the n type current decreases from 8.5 to 3.5 nA with a slope of –0.6 nA kbar^{-1}. The characteristic of the transistor thus evolves from rather p type to a more ambipolar type.

An opposite change of mobility for electrons and holes is excluded since their strain evolution is similar.[43] An improvement of the physical contact with pressure, as described in Ref.[44] is also not expected since it should enhance both n and p channels. Instead we suggest an evolution of the height of the Schottky barrier that is present between the nanotube and the gold contacts.[45,46] The decrease of the p channel (hole current) and the increase of the n channel (electron current) is then consistent with a decrease of the Schottky barrier.

This pressure decrease of the Schottky barrier can actually be quantified from our results. At ambient pressure, the Schottky barrier at the gold–nanotube interface can be estimated to 300 ± 100 meV from the difference of work functions between gold (5.1 eV) and nanotubes (4.8 ± 0.1 eV).[47–49] Then, if we extrapolate the decrease obtained in the inset of Figure 2d, we obtain a perfect ambipolar characteristic ($I_p = I_n$) at 15.4 kbar. At this point, the Schottky barrier is half the energy band gap of the nanotube, which itself is 220 meV, plus or minus 60 meV for its possible pressure evolution.[17] We would thus obtain a Schottky barrier of 110 ± 30 meV at 15.4 kbar. With this extrapolation, we can deduce[50,51] the Schottky barrier pressure derivative in our pressure range: $d\varphi/dP = -12 \pm 8$ meV kbar^{-1}. This large uncertainty comes mainly from the difficulty of perfectly controlling the metal-nanotube interface at the nanoscale. Such a stress dependence of the Schottky barrier has already been reported in other materials, especially in silicon nanowires as an explanation for their piezo-resistive effect.[52] Consistently, it has been predicted that the Shottky barrier at the gold–nanotube contact should decrease with pressure.[53] The invoked mechanism is a hybridizing of the electronic states of gold and the nanotube, resulting in an equalizing of the local work functions at the contacts. Our results thus support this prediction.

More generally, these measurements show that a pressure of 1 GPa can strongly change the characteristics of a transistor made of one individual nanotube, which can be of real interest for applications. In fact, 1 GPa is much less than the pressure that is predicted to be induced by Van der Waals interactions at an inter-tube cross-junction at ambient conditions.[54] Therefore, this kind of effect may take place in some devices and alter the transistor type, especially when a nanotube transistor is almost ambipolar, i.e., based on a small gap semiconducting nanotube.

As a last point, we can study the observed variation with pressure of the gate hysteresis. In **Figure 3a** we plot the two hysteresis

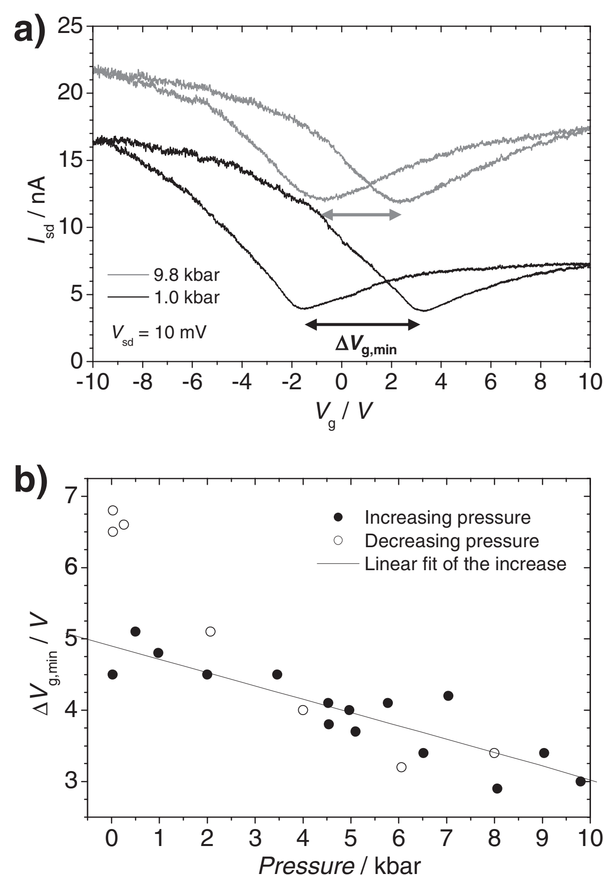

Figure 3. Analysis of the gate voltage hysteresis under pressure. a) Plot of the primary gate voltage characteristics at 1 and 9.8 kbar. This shows the two hysteresis branches that were averaged to obtain Figure 2. The distance between two minima ($\Delta V_{g,min}$) of each curve quantifies the hysteresis amplitude. b) Plot of the hysteresis amplitude ($\Delta V_{g,min}$) with respect to pressure showing a linear and almost reversible decrease.

© 2010 WILEY-VCH Verlag GmbH & Co. KGaA, Weinheim

branches of the I_{sd}–V_g curve at low and high pressure. The evolution of the hysteresis is quantified in Figure 3b by plotting the difference of V_g between the minima of the two hysteresis branches vs. pressure. We observe a decrease of the hysteresis with pressure, increasing again on pressure release. The hysteresis effect is mainly supposed to arise from charge trapping in the surroundings of the nanotube.[55,56] For oxidized silicon substrates, as in our case, the formation of silanol groups on the surface through hydroxylation (Si–O–Si + H_2O → Si–O–H + Si–O–H) has been proposed as a source of protons and electrons screening the gate voltage.[55] If the silanol hypothesis proves to be correct, we might expect the pressure to reverse the equilibrium of the hydroxylation reaction, as observed between silica particles under pressure.[57] The pressure will thus tend to restore a clean silica surface (even if wet) and so reduce the hysteresis. The remaining adsorbed water can then explain the reversibility on pressure release.

3. Conclusions

In summary, we have probed the pressure effects on an ambipolar transistor made of one individual carbon nanotube that proved to be at least double walled, with a semiconducting outer shell and a metallic inner shell. The observed effects of pressure are: i) a strong increase of the current coming from the inner metallic tube, with a change of slope associated to the cross-section transition of the outer tube; ii) a symetrization of the I_{sd}–V_g curve, attributed to a local equalizing of the work functions of gold and the nanotube at the contact; and, iii) a decrease of the gate hysteresis. All these effects are almost fully reversible, and we suggest that they can be used to design sensitive pressure sensors based on one individual nanotube. In particular, the possibility of using the tube cross-section transition to develop pressure sensors is now experimentally proven, even though not exactly as expected.[25] We also give evidence that pressure can have a strong effect on the transistor type, which may be taken into account even for ambient pressure devices because of the Van der Vaals-induced pressure at the contacts. Finally, we propose a scenario for the pressure-induced hysteresis decrease that may confirm the role of silanol groups in the hysteresis. To our knowledge, this is the first time an individual contacted nanotube has been probed under high hydrostatic pressure, or more generally that transport is done through any individual nanosystem under pressure. All these results confirm the interest of combining transport and pressure experiments at the individual level. This new technique may also be useful to study a chirality dependence of the nanotube electronic and mechanical properties under pressure.

Acknowledgements

The authors thank the French National Research Agency (ANR) for its financial support through the grant ANR-06-NANO-012–01. They also thank the Lyon Institute of Nanotechnology (INL) where the photolithography was done, and L. Konczewicz for discussions about the pressure setup.

Received: March 18, 2010
Revised: April 29, 2010
Published online: August 4, 2010

[1] Z. Yao, C. L. Kane, C. Dekker, *Phys. Rev. Lett.* **2000**, *84*, 2941.
[2] S. J. Tans, M. H. Devoret, H. Dai, A. Thess, R. E. Smalley, L. J. Geerligs, C. Dekker, *Nature* **1997**, *386*, 474.
[3] S. J. Tans, A. R. M. Verschueren, C. Dekker, *Nature* **1998**, *393*, 49.
[4] R. Martel, T. Schmidt, H. R. Shea, T. Hertel, P. Avouris, *Appl. Phys. Lett.* **1998**, *73*, 2447.
[5] D. S. Lee, J. Svensson, S. W. Lee, Y. W. Park, E. E. Campbell, *J. Nanosci. Nanotechnol.* **2006**, *6*, 1325.
[6] V. Derycke, R. Martel, J. Appenzeller, P. Avouris, *Nano Lett.* **2001**, *1*, 453.
[7] A. Bachtold, P. Hadley, T. Nakanishi, C. Dekker, *Science* **2001**, *294*, 1317.
[8] M. M. J. Treacy, T. W. Ebbesen, J. M. Gibson, *Nature* **1996**, *381*, 678.
[9] S. Iijima, C. Brabec, A. Maiti, J. Bernholc, *J. Chem. Phys.* **1996**, *104*, 2089.
[10] E. W. Wong, P. E. Sheehan, C. M. Lieber, *Science* **1997**, *277*, 1971.
[11] S. T. Purcell, P. Vincent, C. Journet, V. T. Binh, *Phys. Rev. Lett.* **2002**, *89*, 276103.
[12] V. Sazonova, Y. Yaish, H. Ustunel, D. Roundy, T. A. Arias, P. L. McEuen, *Nature* **2004**, *431*, 284.
[13] H. Chiu, P. Hung, H. W. C. Postma, M. Bockrath, *Nano Lett.* **2008**, *8*, 4342.
[14] L. Yang, M. P. Anantram, J. Han, J. P. Lu, *Phys. Rev. B* **1999**, *60*, 13874.
[15] C. Stampfer, T. Helbling, D. Obergfell, B. Schoberle, M. Tripp, A. Jungen, S. Roth, V. Bright, C. Hierold, *Nano Lett.* **2006**, *6*, 233.
[16] K. Jensen, J. Weldon, H. Garcia, A. Zettl, *Nano Lett.* **2007**, *7*, 3508.
[17] R. B. Capaz, C. D. Spataru, P. Tangney, M. L. Cohen, S. G. Louie, *Phys. Stat. Sol. B* **2004**, *241*, 3352.
[18] Y. Xie, Y. Luo, S. Liu, *Acta Phys. Sin.* **2008**, *57*, 4364.
[19] M. Hasegawa, K. Nishidate, *Phys. Rev. B* **2006**, *74*, 115401.
[20] C. Caillier, D. Machon, A. San-Miguel, R. Arenal, G. Montagnac, H. Cardon, M. Kalbac, M. Zukalova, L. Kavan, *Phys. Rev. B* **2008**, *77*, 125418.
[21] R. Heyd, A. Charlier, E. McRae, *Phys. Rev. B* **1997**, *55*, 6820.
[22] P. E. Lammert, P. Zhang, V. H. Crespi, *Phys. Rev. Lett.* **2000**, *84*, 2453.
[23] O. Gülseren, T. Yildirim, S. Ciraci, Ç. Kılıç, *Phys. Rev. B* **2002**, *65*, 155410.
[24] J. Lu, J. Wu, W. Duan, F. Liu, B. Zhu, B. Gu, *Phys. Rev. Lett.* **2003**, *90*, 156601.
[25] J. Wu, J. Zang, B. Larade, H. Guo, X. G. Gong, F. Liu, *Phys. Rev. B* **2004**, *69*, 153406.
[26] R. S. Deacon, K. Chuang, J. Doig, I. B. Mortimer, R. J. Nicholas, *Phys. Rev. B* **2006**, *74*, 201402.
[27] M. Monteverde, M. Núñez-Regueiro, *Phys. Rev. Lett.* **2005**, *94*, 235501.
[28] M. Paillet, V. Jourdain, P. Poncharal, J. Sauvajol, A. Zahab, J. C. Meyer, S. Roth, N. Cordente, C. Amiens, B. Chaudret, *J. Phys. Chem. B* **2004**, *108*, 17112.
[29] R. Saito, G. Dresselhaus, M. S. Dresselhaus, *Physical Properties of Carbon Nanotubes*, Imperial College Press, London, UK **1998**.
[30] C. L. Kane, E. J. Mele, *Phys. Rev. Lett.* **1997**, *78*, 1932.
[31] T. Yamada, T. Namai, K. Hata, D. N. Futaba, K. Mizuno, J. Fan, M. Yudasaka, M. Yumura, S. Iijima, *Nat. Nanotechnol.* **2006**, *1*, 131.
[32] B. Bourlon, C. Miko, L. Forró, D. C. Glattli, A. Bachtold, *Phys. Rev. Lett.* **2004**, *93*, 176806.
[33] C. Uher, R. L. Hockey, E. Ben-Jacob, *Phys. Rev. B* **1987**, *35*, 4483.
[34] S. Chan, W. Yim, X. G. Gong, Z. Liu, *Phys. Rev. B* **2003**, *68*, 075404.
[35] J. Zang, A. Treibergs, Y. Han, F. Liu, *Phys. Rev. Lett.* **2004**, *92*, 105501.
[36] M. Yao, Z. Wang, B. Liu, Y. Zou, S. Yu, W. Lin, Y. Hou, S. Pan, M. Jin, B. Zou, T. Cui, G. Zou, B. Sundqvist, *Phys. Rev. B* **2008**, *78*, 205411.

© 2010 WILEY-VCH Verlag GmbH & Co. KGaA, Weinheim

[37] J. Arvanitidis, D. Christofilos, K. Papagelis, K. S. Andrikopoulos, T. Takenobu, Y. Iwasa, H. Kataura, S. Ves, G. A. Kourouklis, *Phys. Rev. B* **2005**, *71*, 125404.
[38] V. Gadagkar, S. Saha, D. Muthu, P. K. Maiti, Y. Lansac, A. Jagota, A. Moravsky, R. Loutfy, A. Sood, *J. Nanosci. Nanotechnol.* **2007**, *7*, 1753.
[39] A. L. Aguiar, E. B. Barros, R. B. Capaz, A. G. Souza Filho, P. T. C. Freire, J. Mendes Filho, D. Machon, C. Caillier, Y. A. Kim, M. Muramatsu, M. Endo, A. San-Miguel, *Submitted to Phys.Rev. B.*
[40] T. Hertel, R. E. Walkup, P. Avouris, *Phys. Rev. B* **1998**, *58*, 13870.
[41] D. Christofilos, J. Arvanitidis, G. A. Kourouklis, S. Ves, T. Takenobu, Y. Iwasa, H. Kataura, *Phys. Rev. B* **2007**, *76*, 113402.
[42] J. Arvanitidis, D. Christofilos, G. Kourouklis, S. Ves, T. Takenobu, Y. Iwasa, H. Kataura, *High Pressure Res.* **2009**, *29*, 554.
[43] S. Sreekala, X. Peng, P. M. Ajayan, S. K. Nayak, *Phys. Rev. B* **2008**, *77*, 155434.
[44] I. Ionica, I. Savin, W. Van Den Daele, T. Nguyen, X. Mescot, S. Cristoloveanu, *Appl. Phys. Lett.* **2009**, *94*, 012111.
[45] S. Heinze, J. Tersoff, R. Martel, V. Derycke, J. Appenzeller, P. Avouris, *Phys. Rev. Lett.* **2002**, *89*, 106801.
[46] V. Derycke, R. Martel, J. Appenzeller, P. Avouris, *Appl. Phys. Lett.* **2002**, *80*, 2773.
[47] S. Suzuki, C. Bower, Y. Watanabe, O. Zhou, *Appl. Phys. Lett.* **2000**, *76*, 4007.
[48] X. Cui, M. Freitag, R. Martel, L. Brus, P. Avouris, *Nano Lett.* **2003**, *3*, 783.
[49] P. Liu, Q. Sun, F. Zhu, K. Liu, K. Jiang, L. Liu, Q. Li, S. Fan, *Nano Lett.* **2008**, *8*, 647.
[50] In fact, to be able to extrapolate, we need a linear relationship between the Schottky barrier and I_p–I_n. Calculations based on the following reference, as well as the linear dependence in the inset of Figure 2d, provide strong evidence of this linear relationship.
[51] D. Jimenez, X. Cartoixa, E. Miranda, J. Sune, F. A. Chaves, S. Roche, *Nanotechnology* **2007**, *18*, 25201.
[52] A. C. H. Rowe, *Nat. Nanotechnol.* **2008**, *3*, 311.
[53] N. Park, D. Kang, S. Hong, S. Han, *Appl. Phys. Lett.* **2005**, *87*, 013112.
[54] L. Vitali, M. Burghard, P. Wahl, M. A. Schneider, K. Kern, *Phys. Rev. Lett.* **2006**, *96*, 086804.
[55] J. S. Lee, S. Ryu, K. Yoo, I. S. Choi, W. S. Yun, J. Kim, *J. Phys. Chem. C* **2007**, *111*, 12504.
[56] M. Rinkiö, A. Johansson, G. S. Paraoanu, P. Törmä, *Nano Lett.* **2009**, *9*, 643.
[57] T. M. H. Costa, M. R. Gallas, E. V. Benvenutti, J. A. H. da Jornada, *J. Non-Cryst. Solids* **1997**, *220*, 195.

© 2010 WILEY-VCH Verlag GmbH & Co. KGaA, Weinheim